ISSN 1810-2328, Journal of Engineering Thermophysics, 2024, Vol. 33, No. 2, pp. 303–315. © Pleiades Publishing, Ltd., 2024.

Experimental Investigation of the Heat Transfer under Air or Helium-Xenon Mixture Flow into the Heated 7-Rod Bundle with Spaced Grids

O. V. Vitovsky[1*] and M. S. Makarov[1]

[1] *Kutateladze Institute of Thermophysics, Siberian Branch, Russian Academy of Sciences, Novosibirsk, Russia*

Received November 13, 2023; in final form, May 7, 2024; accepted May 20, 2024

Abstract—The experimental results on heat transfer and pressure drop during the gas coolant flow into a space formed by a dense packing of 7 heated tubes are presented. To fix the tubes rigidly, 8 spacer grids, evenly distributed along the tube lengths, are used together with longitudinal displacers, which ensure a uniform gas flow field in the internal and external channels of the tube bundle. As a working fluid, gas mixtures with a large difference in the Prandtl number were used: air (Pr = 0.7) and helium-xenon mixture (Pr = 0.23). The experiments were carried out in the range of Reynolds numbers of 1926–11200. The wall temperature distributions of the central and peripheral tubes along the length are measured in detail. Particular attention is paid to the areas of gas flow restructuring near the spacer grid. The heat transfer coefficients and friction factors are determined, and the obtained correlations are compared with the known correlations for round channels. The effect of spacer grids, fixing the heated tubes, on local and average heat transfer and friction factors has been analyzed.

DOI: 10.1134/S1810232824020061

1. INTRODUCTION

Heat exchangers, made in the form of a bundle of closely spaced tubes with a coolant flowing along them in-between the tubes, are widely used in chemical production, energy and many other industries. Optimization of the design parameters of these devices, as well as the use of various methods of heat transfer intensification, allow the achievement of economic efficiency of such devices. A nuclear reactor, where the coolant moves in the intertubular space formed by a bundle of cylindrical fuel elements, can be considered as one of applications of such heat exchangers. Nuclear reactors, in which a gas or a mixture of gases is used as a coolant, have a number of advantages over water reactors. These include the possibility of heating the coolant to high temperatures, which increases the power plant efficiency as a whole, as well as the possibility of direct gas output to the turbine in a closed Brayton cycle [1]. An important factor is that the used inert gases and their mixtures are hardly activated in the active zone of the reactor, they are chemically neutral and do not react with the plant materials. The papers [2–4] investigated the physical properties of helium-xenon mixtures and showed the advantages of their use as a coolant in a compact nuclear reactor designed, in particular, to solve various problems of space exploration. The optimal mass concentration of helium in the mixture is from 5 to 10%, while the Prandtl number of the mixture is close to 0.2, which is significantly (3.5 times) lower than that of air.

Features of the nuclear reaction in fuel elements dictate the need for the closest, that is, dense arrangement of round pipes in the reactor volume. In this case, the resulting channels for the flow of the coolant have a complex shape close to quasi-triangular channels. The study of heat transfer during the flow of water and mercury in channels formed by a dense packing of heated rods was carried out in [5–7], which showed the unevenness of temperatures along the channel perimeter. Heat transfer and hydraulic characteristics during the flow of freon-12 in a 7-rod bundle with heated tubes were studied in [8] experimentally and using numerical simulation. It is shown that turbulent mixing in a dense bundle of rods is much stronger than previously thought.

*Corresponding author. E-mail: vitovsky@itp.nsc.ru

The main features of non-isothermal gas flow in channels of complex shape, as well as their difference from traditional round channels, are shown in [9]. The study of heat transfer during the gas coolant flow in channels of complex shape formed by closely spaced fuel elements is an important task of choosing and maintaining the optimal temperature regime of a fuel element to ensure safe operation of a nuclear reactor. A comparison of heat transfer in a steady flow of a helium-xenon mixture with Prandtl number Pr = 0.23 and the air flow with Prandtl number Pr = 0.72 is considered in [10]. A numerical study of heat transfer during the flow of a helium-xenon mixture with a low Prandtl number in a tri-lobe channel and comparison of results with correlations for round channels is given in [11]. An experimental study of the heat transfer characteristics of a helium-xenon mixture in a round tube was carried out in [12]. Correlations of friction factors and coefficients of convective heat transfer were derived and recommended. Numerical modeling of heat transfer in a small-sized reactor cooled with a He-Xe mixture, with a demonstration of temperature fields, was carried out in [3]. The influence of the Prandtl number on heat transfer in the region of laminar-turbulent transition in the initial section of the channel and near the quasi-triangular channel outlet when the flow velocities are close to the velocity of sound was experimentally studied in [9]. A high-velocity flow of air and a helium-xenon mixture in round and quasi-triangular heated tubes of a small diameter was studied numerically and experimentally in [13, 14]. The effect of gas compressibility on heat transfer at high flow velocity and significant flow cooling at the channel outlet under the regime of supersonic gas outflow from the channel is noted. For a dense arrangement of heat-releasing tubes in the reactor volume, in which the distance between the tubes is less than 1 mm, spacing or separating grids are used, installed with a certain step along the entire length of the reactor. The spacer grids prevent changes in gaps between the rods, which can be caused by thermal deformation, and keep the intertubular space for the coolant flow uniform. At the same time, spacer grids represent local resistance to flow that change the structure of the flow. Regular circular-ring inserts or turbulators placed in a heated round tube and changing the flow structure and, as a result, intensifying heat transfer, are considered experimentally and numerically in [15, 16] for the air flow and in [17] for the flow of helium-xenon gas mixture. These works show that ring inserts cause an increase in heat transfer from 1.5 to 3 times as compared to heat transfer in a heated tube without inserts. This increases the pressure drop. Heat transfer during the air flow in a rectangular channel with ribs of various shapes is numerically simulated in [18]. It is shown there that the rib shape affects strongly the distribution of the heat transfer coefficient between the ribs. The hydrodynamic features of the gas flow behind a step in characteristic regions of the separated flow are studied in [19, 20]. The patterns of vortex formation behind a rib and the attachment line coordinate are determined by visualizing the flow. It is shown that a highly turbulent oncoming flow noticeably intensifies local heat transfer behind an obstacle, while the smaller obstacles are more promising heat transfer intensifiers.

The purpose of this work was an experimental study of heat transfer during the flow of air and a helium-xenon mixture of gases in a space formed by seven closely spaced heated tubes with spacer grids uniformly distributed along the length of the tube bundle.

2. INVESTIGATION OF HEAT TRANSFER DURING A GAS FLOW IN A 7-ROD BUNDLE OF HEATED TUBES

2.1. Experimental Equipment

A working section, whose scheme is shown in Fig. 1, was made to perform an experimental study of heat transfer. The total length of the tube bundle is 1084 mm. The diameter of tubes of the bundle is $D = 12.85$ mm. Wall thickness of all tubes $\delta = 0.5$ mm. Thin-walled nichrome tubes made it possible to use electric current to heat the coolant. To supply electric current, brass current-carrying inserts 4 mm wide were used, pressed at each end of the tube. On the gas inlet side, the current-carrying inserts are recessed to a distance of 80 mm. Thus, an unheated initial section 80 mm long was formed to stabilize the flow in the tube bundle and a heated section 1004 mm long. To reduce the current strength, all 7 tubes of the bundle are connected in a series circuit and the input terminal is located at the end of the central tube, the output terminal is at the end of one of the peripheral tubes, which made it possible to implement a constant heat flux from the heated tube walls to the gas.

To obtain rigid fixation of tubes at an equidistant distance from each other, 8 spacer grids, combined with couplings with longitudinal displacers made of heat-resistant UV-curable plastic by

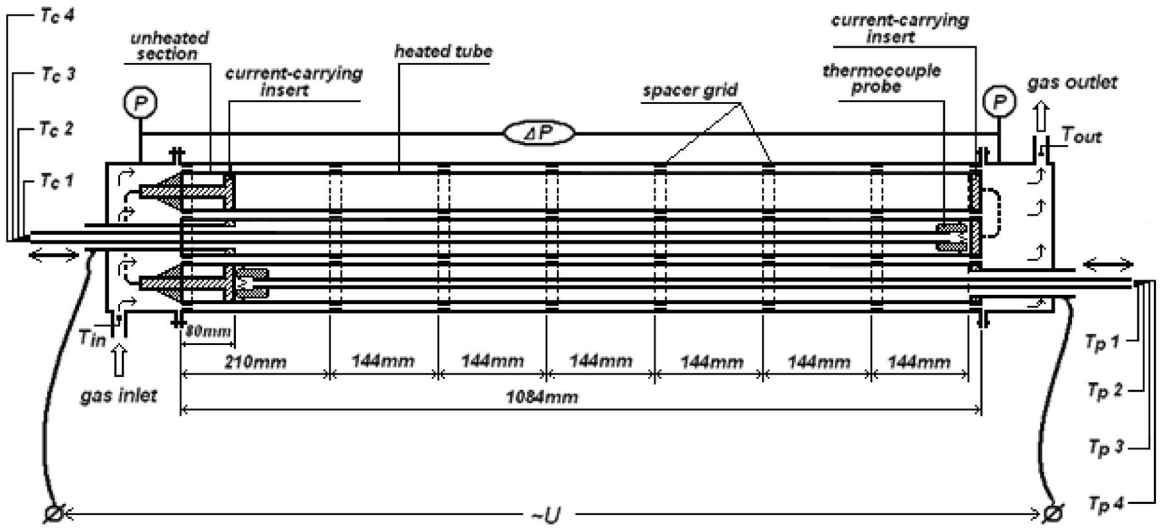

Fig. 1. Working section scheme.

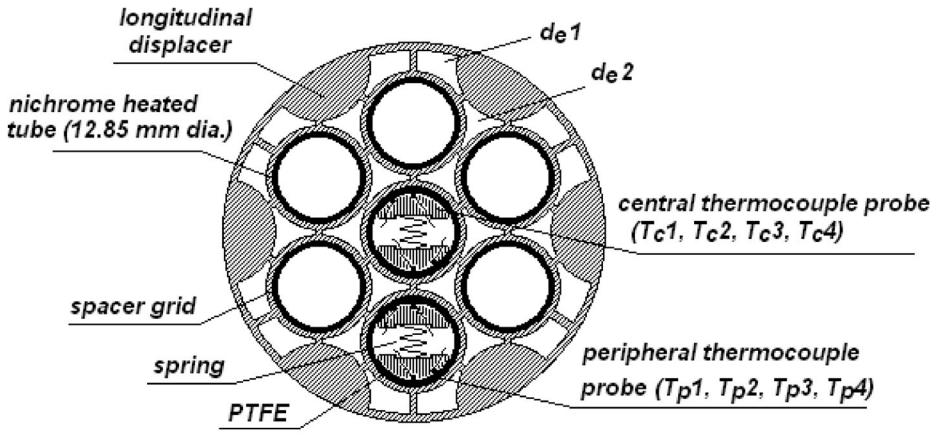

Fig. 2. Cross-section of the working area.

SLA 3D printing, are used. The grids of 10-mm width are located at distances of 0, 210, 354, 498, 642, 786, 930, and 1074 mm from the bundle beginning. The grid walls are 0.95 mm thick. The grids together with displacers are made in such a way that the equivalent diameters of channels between the heated tubes inside the bundle and diameters of the peripheral channels between the heating tubes and the glass wall are equal. The equivalent diameters of various channels of the grid (d_{e1}, d_{e2}) are also equal to each other. This allows the achievement of a uniform field of gas flow rates in the inner and outer channels of the tube bundle.

The distance between the heated tubes was 1.9 mm. Hydraulic diameter of the intertubular channel is $d_h = 5.4$ mm. The cross-section of the tube bundle in the grid zone is shown in Fig. 2.

A general view of a heated tube bundle with spacer grids and couplings with longitudinal displacers is shown in Fig. 3. The construction was placed in a cylindrical housing with the inlet and outlet chambers for gas input/output, where the inlet/outlet pressure and temperature were measured. One end of the central heating tube and one end of a single peripheral tube are open and extend beyond the inlet and outlet chambers, as it is shown in Fig. 1. The wall temperature distribution along the heated tubes is measured through these open ends using movable thermocouple probes.

The thermocouple probe is made of PTFE in the form of a partially cut cylinder fixed on a tube 6 mm in diameter and move freely inside a heated nichrome tube with an inner diameter of

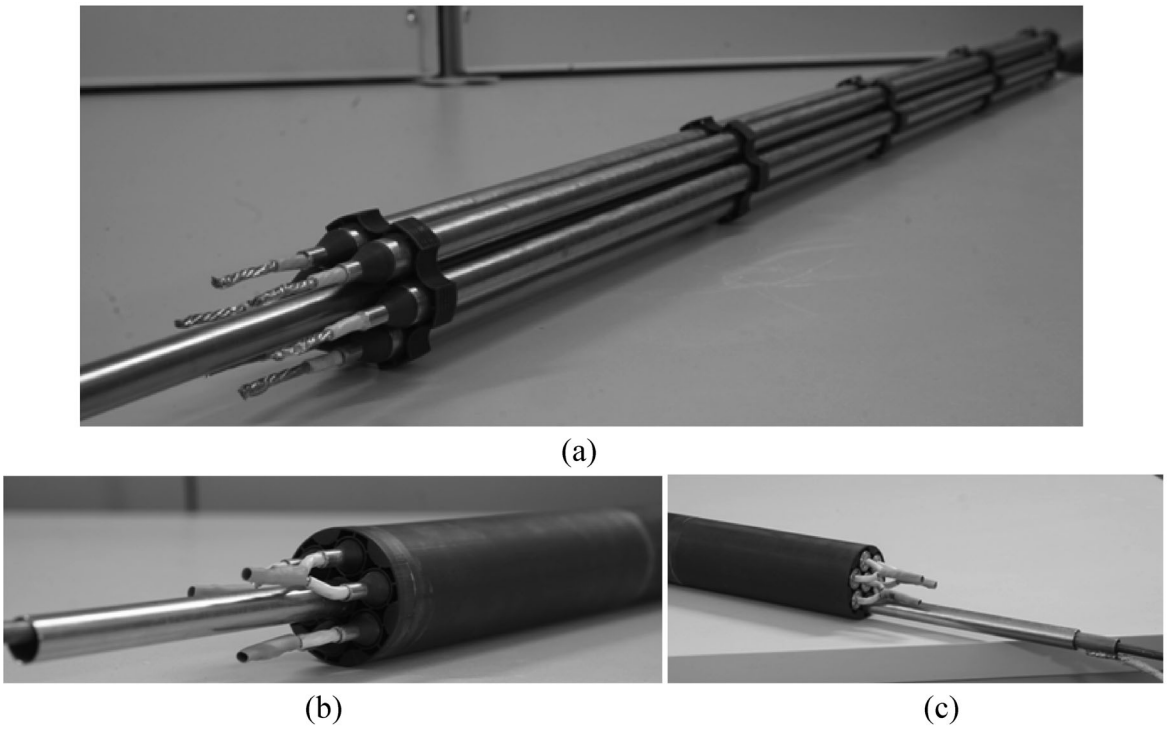

Fig. 3. (a) General view of tube bundle with spacer grids, (b), (c) inlet and outlet ends of tube bundle assembled with couplings and longitudinal displacers, respectively.

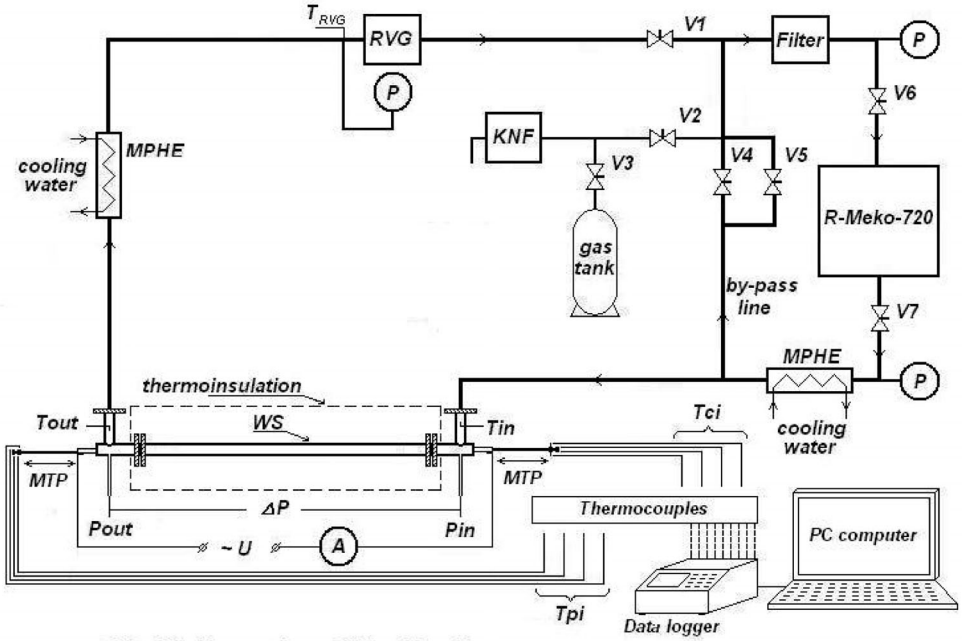

Fig. 4. Scheme of a gas circuit with a working section.

11.85 mm. Four copper-constantan thermocouples (uncertainty of 0.2 K) with a bead diameter of 90 μm, whose ends extend through the tube with a 6-mm diameter, are fixed at a distance of 2.5 mm from the cylinder end in the cut area. The spring, located in the cut area, securely presses thermocouples against the inner wall of the heated tube. The location of thermocouples in relation to adjacent heated tubes is shown in Fig. 2. Thermocouples 1c, 3c, 1p, and 3p are located in the narrowest and thermocouples 2c, 4c, 2p, and 4p are in the widest channels of the tube bundle. The thermocouple probe can be not only moved longitudinally over the entire length of the heated tube, but also rotated to measure the wall temperature distribution along the tube circumference.

The working section is located in a closed gas circuit, where gas circulation is organized by an R-Meko membrane compressor, Fig. 4. The gas temperatures at the inlet T_{in} and at the outlet T_{out} are measured with K-type insulated junction thermocouples (uncertainty of 0.4 K). The absolute pressure in the gas at the inlet and outlet is measured with standard pressure gauges (rated accuracy of 0.15% FS). The pressure drop between the inlet and the outlet is measured using a sapphire pressure transducer (rated accuracy of 0.075% FS). The gas volume flow is measured using a RABO (Elster) rotary gas meter (rated accuracy of 1.5% Rd). Air with a Prandtl number Pr = 0.71 and a helium-xenon mixture with a helium mass concentration of 7.3% (Prandtl number Pr = 0.23) were used as the working fluid.

2.2. Results and Discussion of Heat Transfer under Gas Flow into the Heated 7-Rod Bundle

2.2.1. Temperature Measurements

Figure 5 shows the results of temperature measurements along the wall of the central (T_c) and peripheral (T_p) heated tubes of the bundle during the flow of helium-xenon mixture (a) and air (b) for Reynolds numbers Re = 8240 and 8926, respectively. The Reynolds number is defined as Re = $Gd_h/A\mu$. Here: G is the mass velocity of gas; A and d_h are the cross-sectional area and hydraulic diameter of the bundle channels, μ is the gas dynamic viscosity. Measurements for Fig. 5 are drawn with a step of 20 mm.

More details with a step of 5 mm in Fig. 6 show the results of measuring the temperature of the wall of the central (T_c) heated tube of the bundle during the flow of helium-xenon mixture (a) and air (b) for Reynolds numbers Re = 5397 and 5257, respectively, between the separation grids in the middle of the channel. The black solid line in Fig. 5 shows a change in the gas temperature from the working section inlet to the outlet.

The gas temperature distribution along the length of the working section reflects the average temperature value for all channels and is obtained by linear temperature interpolation from the inlet (T_{in}) to the outlet (T_{out}). Vertical dashed lines indicate the spacer grid positions in the working section. The results of temperature measurements presented in Figs. 5 and 6 demonstrate a periodic increase in the tube wall temperature when approaching the spacer grid and a decrease in temperature behind the grid. With an increase in the gas flow rate, a change in the tube wall temperature before the grid and behind it becomes more intense. With an increase in the gas flow rate, there is a grow in the temperature change of the tube wall up to the grid and behind it. The observed temperature behavior is explained by the following two circumstances. Firstly, the flow area of the quasi-triangular channel of the spacer grid is 3.17 times smaller than the flow area of the corresponding annular channel suitable for the grid. This leads to the fact that the gas flow slows down in front of the grid wall (before the ledge) and accelerates when passing through the cross section of the passage section within the spacer grid. The second circumstance is that the grid wall 0.95 mm thick and 10 mm long, adjacent to the tube, is an obstacle to the gas flow and, as in the case of gas flow in channels with transverse ribs [19–21], a vortex flow structure develops behind the step in the recirculation region. The intensity of recirculation increases with increasing flow velocity The size of the recirculation region or the location of the reattachment line, where the wall temperature is minimal behind the grid and from which the formation of a new boundary layer begins, as is known, weakly depends on the Reynolds number and amounts to 10–15 obstacle heights, which is agreement with data in Fig. 6.

The presence of grids along the tubes leads to periodic destruction and growth of hydrodynamic and thermal boundary layers, the ratio between the thicknesses of which is determined by the value of the Prandtl number. The observed change in the wall temperature in the region of the grid during

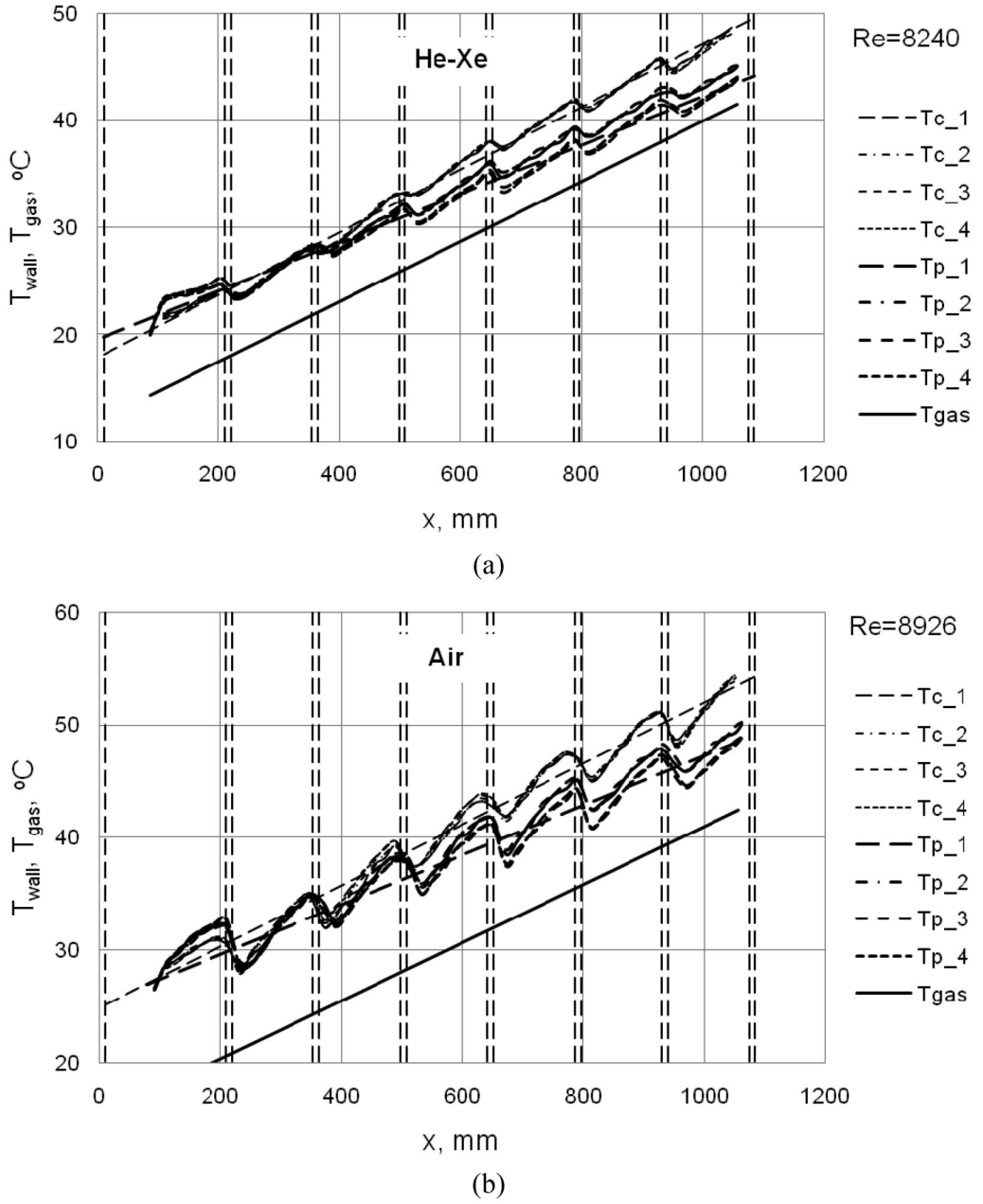

Fig. 5. Distribution of the wall temperature of the central and peripheral tubes and the temperature of gas along the length of the 7-rod bundle for helium-xenon mixture (a) and air (b) at Reynolds numbers Re = 8240 and Re = 8926, respectively.

the flow of a helium-xenon mixture with the Prandtl number Pr = 0.23 ($\sim$ 1.5 K) and during the air flow with the Prandtl number Pr = 0.71 ($\sim$ 3 K). This fact indicates a greater thermal inertia of the helium-xenon coolant compared to air. The dynamic boundary layer, which collapses when overcoming an obstacle, is sunk in the thermal boundary layer for this coolant, and, as a result, has a lesser effect on the temperature field near the wall. For air, the destruction of the dynamic boundary layer is accompanied by a similar destruction of the thermal boundary layer, and the temperature field actually tracks the dynamics of the flow.

It can be noted that for air in the area of the grid location and the adjacent recirculation area, a monotonous decrease in the temperature of the tube wall in the direction of flow is observed, that is, an increase in local heat transfer, while when a vortex is formed in the recirculation area, the heat transfer intensity should decrease and the wall temperature should increase. For a helium-

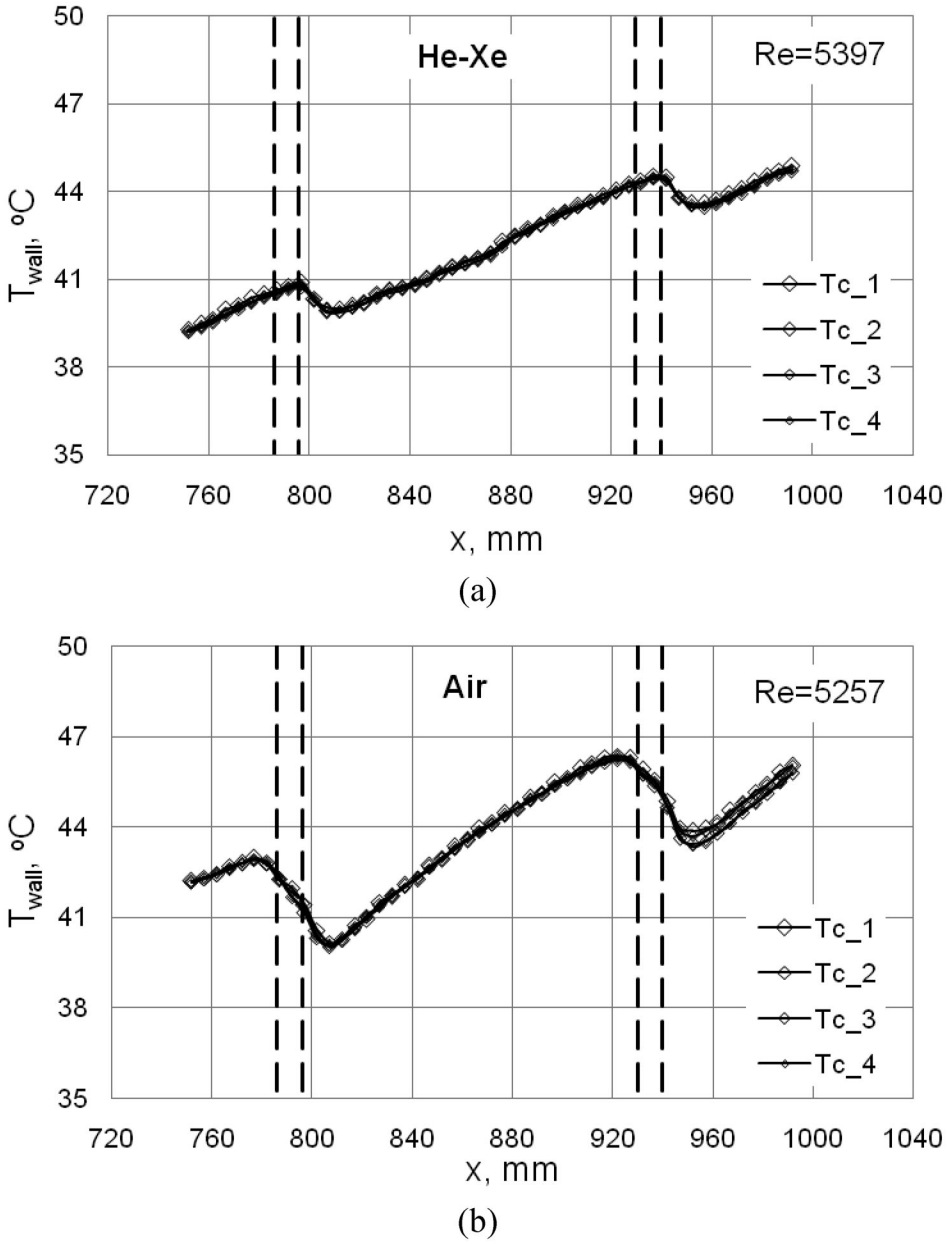

Fig. 6. Distribution of the wall temperature of the central tube in the area between the separation grids for helium-xenon mixture (a) and air (b) at Reynolds numbers Re = 5397 and Re = 5257, respectively.

xenon mixture, such a picture is not observed; the wall temperature decreases only near the flow reattachment line after separation behind the step.

The previously noted strong connection between the thermal and dynamic boundary layers in the air flow and, on the contrary, the weak connection in the helium-xenon mixture flow allows us to explain the difference in the wall temperature distribution in this region. When the coolant passes through the grid channel, which has a flow area that is more than 3 times smaller than the cross-section of the inter-tube channel, the local flow velocity, respectively, increases, which leads to an increase in local heat transfer in the area of the grid location and the air recirculation area. Due to thermal inertia, local heat transfer in the helium-xenon mixture flow does not have time to change significantly within the lattice rib, and changes only in the recirculation region.

The distribution of the wall temperature of the central and peripheral heated tubes shows that the temperature of the wall of the central tube exceeds the temperature of the walls of the peripheral tubes, increasing in the direction of the gas outlet from the working section. Near the outlet, this

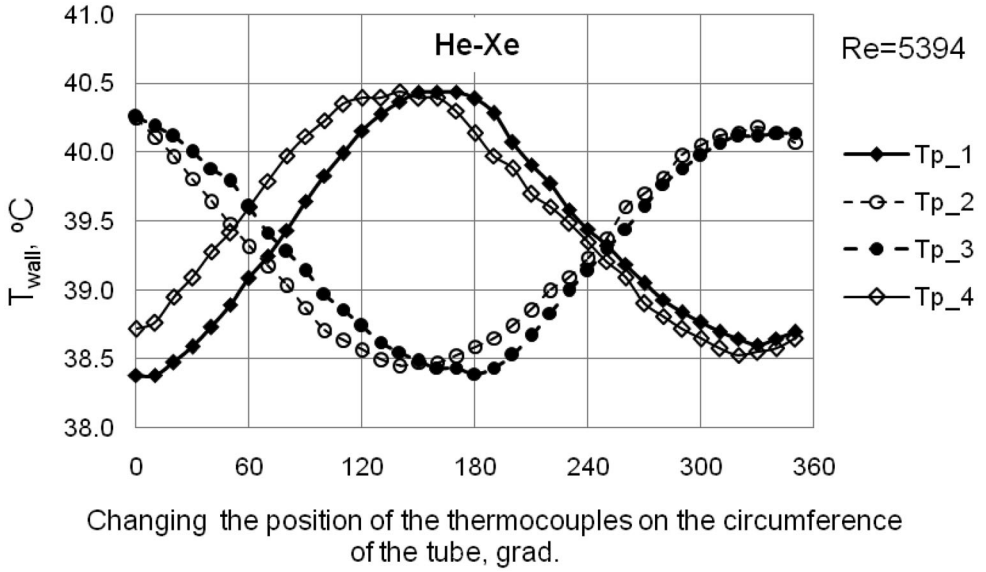

Fig. 7. A change in the wall temperature along the circumference of the peripheral tube during the flow of helium-xenon coolant at $x = 747$ mm and Reynolds number Re = 5394.

difference is 1–2 K at low Reynolds numbers, reaching values of 5–6 K at high Reynolds numbers, i.e., it increases with increasing gas flow. This is due to the fact that the walls of the quasi-triangular channels around the central tube give off heat from all three sides, while the peripheral quasi-triangular channels and channels along the bounding unheated wall give off heat from both sides. This leads to the fact that the temperature of the gas in the central channels rises more than the temperature of the gas in the peripheral channels, and the temperature of the wall of the central tube, respectively, is higher than the temperature of the walls of the peripheral tubes. The distribution of the wall temperature along the circumference of the peripheral tube at the point with the coordinate $x = 747$ mm for the flow of a helium-xenon coolant with the Reynolds number Re = 5394 is shown in Fig. 7. In the initial position, thermocouple T_{p1} is located at the point with the smallest distance from the central heated tube, and thermocouple T_{p3}, respectively, at the point of greatest distance from the central heated tube near the unheated wall. During further measurements, the thermocouples moved along the circumference of the pipe with a step of 10°. The temperature difference between opposite thermocouples reaches ~ 2 K, which is also observed in Fig. 5. It should be noted that there is no significant difference in the temperature of the tube wall in the narrow and wide parts of the gas channel (shift in the azimuth of the tube is 30°). This is in good agreement with the results of [10], where it is shown that the thermal conductivity of even a thin wall of a heated triangular channel leads to a smoothing of the wall temperature distribution from the corner to the center of the channel.

2.2.2. Friction Factor under Gas Flow into 7-Rod Bundle

For processing experimental data, the friction factor is defined as:

$$f = \frac{\Delta P}{L}\frac{2d_h}{\rho V^2}. \tag{1}$$

Here ΔP is the pressure drop in the working section, L is the tube length in the working section, ρ and V are the average values of density and average flow rate of gas between the inlet and outlet, respectively. Dependence of the friction factor on the Reynolds number, obtained in the experiments, is shown in Fig. 8 by round dots for the helium-xenon mixture and diamonds for air. The dotted line shows the approximation of the experimental data. The black dashed line in Fig. 8 shows the correlation of the friction factor given in [21] for a bundle of rods with a triangular arrangement, in the form

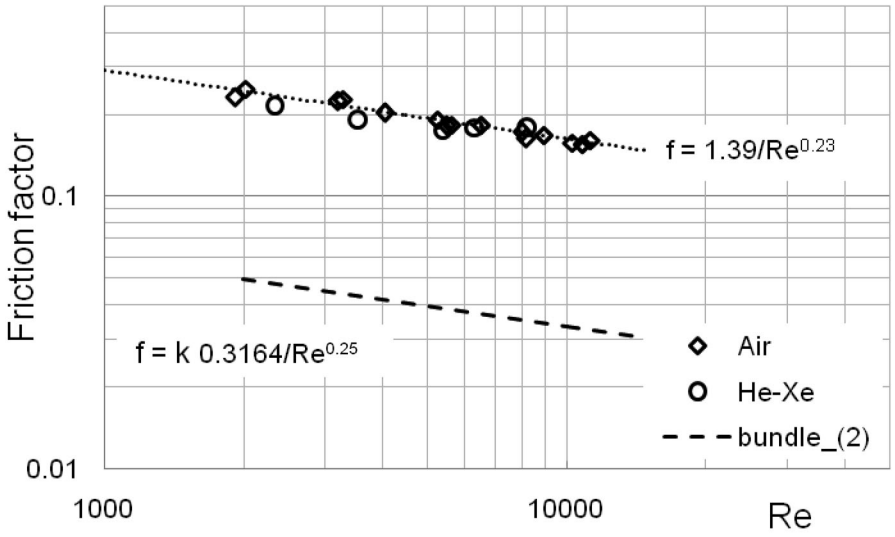

Fig. 8. Friction factor vs. Reynolds number.

$$f = k0.3164\ \mathrm{Re}^{-0.25},$$

$$k = 0.57 + 0.18(s-1) + 0.53[1 - \exp(-a)], \tag{2}$$

$$a = 0.58 + 9.2(s-1).$$

Here $s = b/D$, where b is the distance between the central axes of tubes in the bundle, D is the outer diameter of the tubes.

The observed almost 5-fold increase in the friction factor in a 7-rod bundle of tubes with spacer grids as compared to the correlation obtained for the rod bundle without grids is explained by the presence of periodic local resistance associated with a sharp constriction of the flow when it passes through the grid channels. These resistances lead to an increase in the pressure drop along the length of the tubes, which, accordingly, leads to an increase in the friction factor.

As noted above and as shown in Fig. 6, behind the grid, the dynamic boundary layer is torn off and a new boundary layer is formed from the reattachment line. The length of this initial hydrodynamic section is commensurate with the distance between adjacent grids. This circumstance also leads to an increase in the total pressure drop.

2.2.3. Heat Transfer Correlation for 7-Rod Bundle

The dimensionless heat transfer coefficient in the form of Nusselt number is defined as:

$$Nu = \alpha d_h/\lambda. \tag{3}$$

Here d_h is the hydraulic diameter of the 7-rod tube bundle, λ is the thermal conductivity of the coolant. The heat transfer coefficient α is defined as:

$$\alpha = \frac{Q}{S(\overline{T}_w - \overline{T}_g)}. \tag{4}$$

Here Q is the heat released on tubes determined as $Q = U^*I$, where U is the voltage, I is the strength of current, S is an open surface of the heated tubes. The average wall temperature $\overline{T}_w$ is defined as

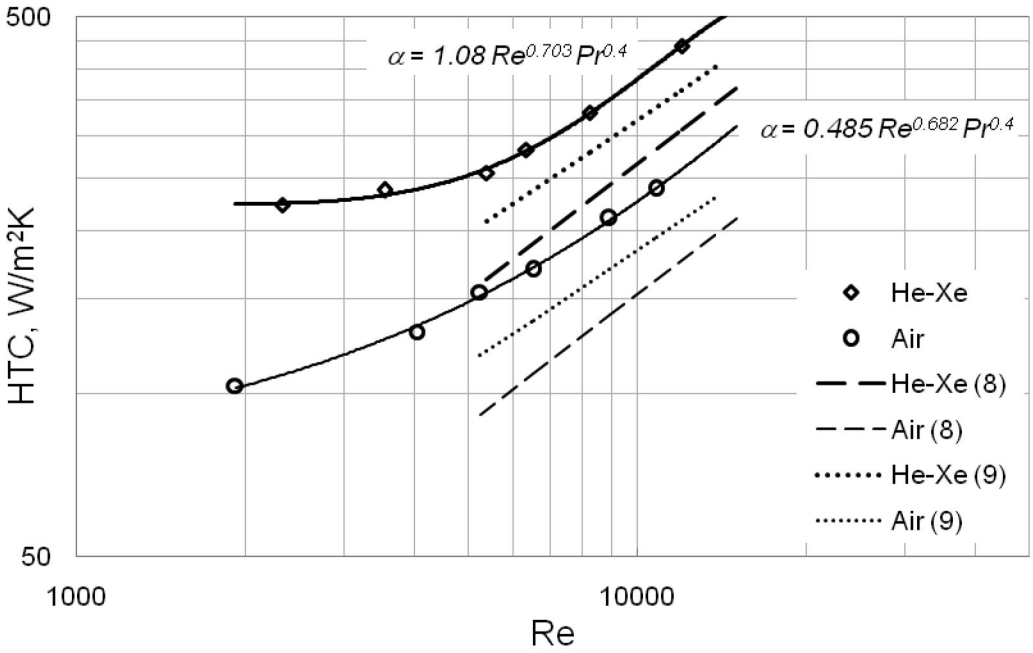

Fig. 9. Heat transfer coefficients vs. Reynolds number.

$$\overline{T}_w = \frac{\overline{T}_{c,w} + 6\overline{T}_{p,w}}{7}. \tag{5}$$

Here $\overline{T}_{c,w}$ is the average temperature of the central tube wall, determined after linear approximation of all four distributions of the wall temperature along the length in the middle of the tube heated region with coordinate $x = 565$ mm, $\overline{T}_{p,w}$ is the average temperature of the peripheral tube wall determined in the same manner. The average wall temperatures of the central and peripheral tubes are shown in Figs. 5 and 6 by thick and thin dashed lines, respectively. The average gas temperature $\overline{T}_g$ is determined as the average gas temperature from the working section inlet to its outlet $\overline{T}_g = (T_{g,in} + T_{g,out})/2$.

Comparison of heat transfer to the flow of gases with different thermal conductivity should be carried out using the dimensional heat transfer coefficients α. Figure 9 shows the dependences of the heat transfer coefficient on the Reynolds number for the flow of helium-xenon coolant (diamonds) and air (round dots). The thick and thin solid lines show the corresponding approximations of the experimental data. With a decrease in the Reynolds number (Re $<$ 5500), a transition of the flow to a laminar regime is observed, at which the heat transfer coefficient tends to a constant value. In the region of turbulent flow at high Reynolds numbers (Re $>$ 5500), the experimental data are described by a dependence of the form

$$\alpha = 1.08\mathrm{Re}^{0.703}\mathrm{Pr}^{0.4} \tag{6}$$

during the flow of helium-xenon mixture and

$$\alpha = 0.485\mathrm{Re}^{0.682}\mathrm{Pr}^{0.4} \tag{7}$$

during air flow.

For comparison, in Fig. 9, the thick (helium-xenon mixture) and thin (air) dashed lines show the heat transfer coefficients calculated using the Dittus–Boelter correlation [22] obtained for a stabilized turbulent gas flow in a round tube in the form

$$\alpha = \frac{\lambda}{d_h} 0.023 \mathrm{Re}^{0.8} \mathrm{Pr}^{0.4}. \quad (8)$$

The dotted thick (helium-xenon mixture) and thin (air) lines show the heat transfer coefficients calculated using the correlation obtained by the authors [15] when studying heat transfer during air flow in a heated round tube with ring turbulators in the form

$$\alpha = \frac{\lambda}{d_h} 0.354 \mathrm{Re}^{0.697} \mathrm{Pr}^{0.4} (d_{h,g\text{к}}/d_h)^{-0.555} (l_{g\text{к}}/d_h)^{-0.598}. \quad (9)$$

Here $d_{h,gr}, d_h$ are the hydraulic diameters of the grid flow channel and the 7-rod tube bundle, l_{gr} is the distance between the grids.

An increase in the heat transfer coefficient in the 7-rod bundle by 1.4–1.6 times as compared with a smooth round channel can be explained by the same reasons, which cause an increase in heat transfer when air flows in a heated round tube with circular-ring turbulators noted in [15, 16]. Spacer grids, which provide fixation of heated tubes in a 7-rod assembly, like annular turbulators in a tube, lead to a limited growth of the boundary layer due to its periodic destruction in the separation zone behind the rib. And, as is known, the heat transfer in the initial section is much higher than in the region of steady flow. Another reason for the increase in heat transfer is the formation of vortex structures behind the grid, which was also noted in [16–19]. The similarity of heat transfer intensification mechanisms in a 7-rod assembly with spacer grids and in a round tube with annular turbulators is also indicated by close values of the exponent at the Reynolds number in the obtained experimental correlations for the heat transfer coefficient. The absence of stabilized flow regions caused by closely spaced spacer grids in the channels of the 7-rod assembly does not allow the use of well-known correlations, Dittus–Boelter, Petukhov, etc., to predict heat transfer and requires numerical simulation of the flow and heat transfer in such channels.

CONCLUSIONS

The heat transfer and hydraulic resistance during the flow of a helium-xenon mixture with a small Prandtl number and air in the space formed by a 7-rod bundle of heated tubes was experimentally studied. The influence of grids fixing heated tubes on the surface temperature distribution of both central and peripheral tubes was analyzed. It is shown that there is a periodic increase in the temperature of the tube wall when approaching the spacer grid and a decrease in the temperature behind the grid. Periodic destruction and growth of hydrodynamic and thermal boundary layers, as well as separation of the flow and formation of a vortex behind the spacer grid leads to the intensification of heat transfer. The presence of periodic local resistances associated with a sharp narrowing of the flow when it passes through the channels of the grids leads to an increase in the pressure drop along the length of the tubes, which, accordingly, causes an increase in the friction factor. The results of the work are of great importance for the design of power plants with a gas coolant.

NOTATIONS

A—channel cross-sectional area (m^2)
b—distance between the central axes of tubes
D—external diameter of tube (m)
d—diameter (m)
I—electric current (A)
G - mass flow rate (kg/s)
L—tube length (m)
Nu—Nusselt number
P—pressure (bar)
Pr—Prandtl number
Q—heat load (W)

Re—Reynolds number
S—inner surface of the heated tubes (m^2)
T—temperature (°C)
U—electric voltage (V)
V—velocity (m/s)
x—distance from the inlet (m)

Greek Symbols

α—heat transfer coefficient (W/m^2K)
δ—wall thickness of tube (m)
λ—thermal conductivity (W/m k)
ρ—density (kg/m^3)
μ—dynamic viscosity (Pa s)

Subscripts

c—central
e—equivalent
h—hydraulic
g—gas
gr—grid
in—inlet
out—outlet
p—peripheral
w—tube wall

FUNDING

This work was supported by ongoing institutional funding. No additional grants to carry out or direct this particular research were obtained.

CONFLICT OF INTERESTS

The authors of this work declare that they have no conflicts of interest.

REFERENCES

1. Khan, M.S., Bai, Y., Huang, Q., Xu, C., Sun, L., and Zou, X., Conceptual Design and Optimization of Power Generation System for Lead-Based Reactor, *Appl. Therm. Eng.*, 2020, vol. 168, p. 114714; http://doi.org/10.1016/j.applthermaleng.2019.114714
2. El-Genk, M.S.and Tournier, J-M., Noble-Gas Binary Mixtures for Closed-Brayton-Cycle Space Reactor Power Systems, *J. Propul. Power.*, 2007, vol. 23, 863–873; https://doi.org/10.2514/1.27664
3. Meng, T., Cheng, K., Zhao, F., Xia, C., and Tan, S., Computational Flow and Heat Transfer Design and Analysis for 1/12 Gas-Cooled Space Nuclear Reactor, *Ann. Nucl. Energy*, 2020, vol. 135, p. 106986; DOI:10.1016/j.anucene.2019.106986
4. Mazzetti, A., Gianotti Pret, M., Pinarello, G., Celotti, L., Piskacev, M., and Cowley, A., Heat to Electricity Conversion Systems for Moon Exploration Scenarios: A Review of Space and Ground Technologies, *Acta Astronaut.*, 2019, vol. 156, pp. 162-186; DOI:10.1016/j.actaastro.2018.09.025
5. Subbotin, V.I., Ushakov, P.A., Gabrianovich, B.N., and Zhukov, A.V., Heat Exchange during the Flow of Mercury and Water in a Tightly Packed Rod Pile, *Sov. Atom Energy*, 1961, pp. 1001–1009.
6. Bobkov, V.P., Ibragimov, M.K., Sinyavskii, V.F., and Tychinskii, N.A., Heat Exchange for Flow of Water in a Densely Packed Triangular Bundle of Rods, *Sov. Atom Energy*, 1974, vol. 37, 823–827.
7. Koshkin, V.K., Kalinin, E.K., Yarkho, S.A., and Ter-Mkrtchjan, A.A., Heat Transfer in the Channel of Dense Packing of a Bundle of Pipes or Rods, *High Temp.*, 1967, vol. 5, 317–321.
8. Cheng, X. and Yu, Y.Q., Local Thermal-Hydraulic Behavior in Tight 7-Rod Bundles, *Nucl. Engng. Des.*, 2009, vol. 239, pp. 1944–1955; DOI:10.1016/j.nucengdes.2009.04.010

9. Vitovsky, O.V., Experimental Study of Heat Transfer during the Flow of a Gas Coolant in a Heated Quasi-Triangular Channel, *Int. J. Heat Mass Transfer*, 2022, vol. 190, p. 122771; DOI:10.1016/j.ijheatmasstransfer.2022.122771
10. Vitovsky, O.V., Elistratov, S.L., Makarov, M.S., Nakoryakov, V.E., and Naumkin, V.S., Heat Transfer in a Flow of Gas Mixture with Low Prandtl Number in Triangular Channels, *J. Eng. Therm.*, 2016, vol. 25, pp. 15–23.
11. Qin, H., Fang, Y., Wang, C., Tian, W., Qiu, S., Su, G., and Deng, J., Numerical Investigation on Heat Transfer Characteristics of Helium-Xenon Gas Mixture, *Int. J. Energy Res.*, 2021, vol. 45, pp. 11745–11758; DOI: 10.1002/er.5692
12. Qin, H., Wang, C., Tian, W., Qiu, S., and Su, G., Experimenal Investigation on Flow and Heat Transfer Characteristics of He-Xe Gas Mixture, *Int. J. Heat Mass Transfer*, 2022, vol. 192, p. 122942; DOI:10.1016/j.ijheatmasstransfer.2022.122942
13. Vitovsky, O.V., Makarov, M.S., Nakoryakov, V.E., and Naumkin, V.S., Heat Transfer in a Small Diameter Tube at High Reynolds Number, *Int. J. Heat Mass Transfer*, 2017, vol. 109, pp. 997–1003; DOI:10.1016/j.ijheatmasstransfer.2017.02.041
14. Makarov, M.S., Vitovsky, O.V., Naumkin, V.S., and Lebeda, K.S., Investigation of Hydraulic Resistance and Heat Transfer in the Flow of He-Xe Mixture with a Small Prandtl Number in a Quasi-Triangular Pipe, *Int. J. Heat Mass Transfer*, 2022, vol. 199, p. 123427; DOI:10.1016/j.ijheatmasstransfer.2022.123427
15. Kongkaitpaiboon, V., Nanan, K., and Eiamsa-ard, S., Experimental Investigation of Convective Heat Transfer and Pressure Loss in a Round Tube Fitted with Circular-Ring Turbulators, *Int. Commun. Heat Mass Transfer*, 2010, vol. 37, pp. 568–574; DOI:10.1016/j.icheatmasstransfer.2009.12.016
16. Ruengpayungsak, K., Wongcharee, K., Thianpong, C., Pimsarn, M., Chuwattanakul, V., and Eiamsa-ard, S., Heat Transfer Evaluation of Turbulent Flows through Gear-Ring Elements, *Appl. Therm. Eng.*, 2017, vol. 123, pp. 991–1005; http://dx.doi.org/10.1016/j.applthermaleng.2017.05.108
17. Shi, X., Wang, L., Chen, W., Li, Z., Chai, X., and Chyu, V.K., Effect of Induced Vortex and Configuration Layout on Heat Transfer Enhancement of Helium-Xenon Mixture, *Appl. Therm. Eng.*, 2023, vol. 225, p. 120168; http://doi.org/10.1016/j.applthermaleng.2023.120168
18. Kamali, R. and Binesh, A.R., The Importance of Rib Shape Effects on the Local Heat Transfer and Flow Friction Characteristics of Square Ducts with Ribbed Internal Surfaces, *Int. Commun. Heat Mass Transfer*, 2008, vol. 35, pp. 1032–1040; DOI:10.1016/j.icheatmasstransfer.2008.04.012
19. Terekhov, V.I., Yarygina, N.I., and Zhdanov, R.F., Heat Transfer in Turbulent Separated Flows in the Presence of High Free-Stream Turbulence, *Int. J. Heat Mass Transfer*, 2003, vol. 46, 4535–4551; DOI:10.1016/S0017-9310(03)00291-6
20. Smulsky, Ya.I., Terekhov, V.I., and Yarygina, N.I., Heat Transfer in Turbulent Separated Flow behind a Rib on the Surface of Square Channel at Different Orientation Angles Relative to Flow Direction, *Int. J. Heat Mass Transfer*, 2012, vol. 55, pp. 726–733; DOI:10.1016/j.ijheatmasstransfer.2011.10.037
21. Ushakov, P.A., Calculation of the Hydrodynamic Characteristics of the Longitudinal Flow of Liquid around Regular Arrays of Fuel Element Rods, *High Temp.*, 1074, vol. 12, pp. 89–95.
22. Dittus, F.W. and Boelter, L.M.K., Heat Transfer in Automobile Radiators of Tubular Type, *Int. Commun. Heat Mass Transfer*, 1985, vol. 12, pp. 3–22; https://doi.org/10.1016/0735-1933(85)90003-X